

# Escape rate of metastable states in a driven NbN superconducting microwave resonator

Baleegh Abdo,\* Eran Arbel-Segev, Oleg Shtempluck, and Eyal Buks

*Department of Electrical Engineering, Technion, Haifa 32000, Israel*

(Dated: April 24, 2018)

We study thermal instability and formation of local hot spots in a driven nonlinear NbN superconducting microwave resonator. White noise injected into the resonator results in transitions between the metastable states via a process consisting of two stages. In the first stage, the input noise entering the system induces fluctuations in the resonator mode. While, in the second one, these mode fluctuations result in phase transitions of the hot spot due to induced temperature fluctuations. The associated noise-activated escape rate is calculated theoretically, and also measured experimentally by means of driving the system into stochastic resonance. A comparison between theory and experiment yields a partial agreement.

PACS numbers: 74.40.+k, 02.50.Ey, 85.25.-j

## I. INTRODUCTION

The simple model of noise activated escape of a Brownian particle over a potential barrier successfully explains the basic behavior of a large number of metastable systems in nature<sup>1</sup>. Examples of such systems can be found in almost all major fields of science: physics, chemistry, biology and even engineering<sup>2</sup>. For instance, it explains biochemical reactions in ac-driven protein<sup>3</sup>, the lifetime of zero-voltage state in Josephson junctions<sup>4,5</sup>, the magnetization reversal in nanomagnets<sup>6,7,8</sup>, noise-activated switching in micro<sup>9</sup> and nano<sup>10,11</sup> mechanical oscillators, and photon-assisted tunneling in semiconductor heterostructures<sup>12</sup>.

A well-known pioneering work on the subject is Krammer's in 1940. In his seminal paper<sup>13</sup>, he derived relatively simple expressions for the thermally induced escape rate in a one-dimensional asymmetric double-well potential. In general, these escape rate expressions take the form of  $\Gamma = \Gamma_0 \exp(-U_b/k_B T)$ , where  $U_b$  is the potential barrier height,  $k_B$  is Boltzmann's constant,  $T$  is the temperature (where the limit  $k_B T \ll U_b$  is assumed), and  $\Gamma_0$  is a rate prefactor. Important extensions and refinements to this formula aimed either to include a wider range of damping regimes<sup>14,15,16</sup> or accommodate the solutions to other cases such as nonequilibrium systems, have been contributed by many authors over the years<sup>17,18,19</sup>. Examples of such nonequilibrium systems are metastable potentials modulated by deterministic forces<sup>20</sup> e. g. the case of stochastic resonance<sup>21,22</sup>, or metastable systems subjected to nonwhite noise<sup>23,24</sup>. Moreover, efforts have been invested also in extending Krammer's rate theory to describe metastable systems in the quantum limit<sup>1,25,26</sup>, where escape is dominated by tunneling.

In the present paper we study the escape rate of metastable states of thermally unstable superconducting stripline resonators both theoretically and experimentally. In recent studies<sup>27,28</sup> we have experimentally demonstrated such instability in NbN superconducting resonators. The measured response of the system to a

monochromatic excitation was successfully accounted for by a theoretical model, which attributed the instability to a local hot spot in the resonator, switching between the superconducting and the normal phases. Nonlinearity, according to this model, results due to coupling between the equations of motion for both, the mode amplitude in the resonator and the temperature of the hot spot. The coupling mechanism is based on the dependence of both the resonance frequency and the damping rate of the resonator on the stripline impedance, which in turn depends on the temperature of the hot spot. Moreover, we have employed this instability to demonstrate experimentally intermodulation gain<sup>29</sup>, stochastic resonance<sup>30</sup>, self-sustained modulation of a monochromatic drive<sup>31,32</sup>, period doubling bifurcation, and noise squeezing<sup>33</sup>.

In the case of thermally unstable superconducting stripline resonators, the escape mechanism governing the lifetime of the metastable states differs in general from many of the examples mentioned above. In this case, the input noise induces escape in a two-stage process. The direct coupling between the input noise and the driven mode leads to fluctuations in the mode amplitude, which in turn, induce fluctuations in the heating power applied to the hot spot. Consequently, the fluctuating heating power, which is characterized by a finite correlation time, leads to temperature fluctuations. Escape occurs when the temperature approaches the critical value and a phase transition takes place in the hot spot.

The remainder of this paper is organized as follows. In Sec. II the steady state solutions of the equation of motion for the resonator-mode are derived for the case of local heating instability. In Sec. III a perturbative approach is applied in order to include the effect of thermal fluctuations. In Sec. IV an escape rate expression characterizing the metastable states of the resonator is obtained. In Sec. V a brief explanation regarding stochastic resonance measurement is given. While in Secs. V. A and V. B stochastic resonance measurement results are employed in order to extract some of the transition rate parameters characterizing the system. Finally, a brief summary concludes this paper in Sec VI.

## II. STEADY STATE SOLUTIONS

Consider the case of a superconducting stripline microwave resonator weakly coupled to a feedline. Driving the resonator by a coherent tone  $a_1^{in} = b^{in}e^{-i\omega_p t}$  injected into the feedline, excites a mode in the resonator with an amplitude  $A = Be^{-i\omega_p t}$ , where  $\omega_p$  is the drive angular frequency,  $b^{in}$  is a constant complex amplitude proportional to the drive strength, and  $B(t)$  is a complex mode amplitude which is assumed to vary slowly on the time scale of  $1/\omega_p$ .

### A. Mode Amplitude

In this approximation, the equation of motion for  $B$  reads<sup>34</sup>

$$\frac{dB}{dt} = [i(\omega_p - \omega_0) - \gamma]B - i\sqrt{2\gamma_1}b^{in} + c^{in}, \quad (1)$$

where  $\omega_0$  is the angular resonance frequency,  $\gamma = \gamma_1 + \gamma_2$ , where  $\gamma_1$  is the coupling factor between the resonator and the feedline, and  $\gamma_2$  is the damping rate of the mode. The term  $c^{in}$  represents an input noise with a random phase

$$\langle c^{in} \rangle = 0, \quad (2)$$

and autocorrelation functions given by

$$\langle c^{in}(t)c^{in*}(t') \rangle = \langle c^{in*}(t)c^{in*}(t') \rangle = 0, \quad (3)$$

$$\langle c^{in}(t)c^{in*}(t') \rangle = G\omega_0\delta(t - t'). \quad (4)$$

By further assuming a thermal equilibrium condition at temperature  $T_{\text{eff}}$  and a relatively high temperature case  $k_B T_{\text{eff}} \gg \hbar\omega_0$ , one has

$$G = \frac{\gamma}{\omega_0} \frac{k_B T_{\text{eff}}}{\hbar\omega_0}. \quad (5)$$

Rewriting Eq. (1) in terms of the dimensionless time  $\tau = \omega_0 t$  and using the steady state solution

$$B_\infty = \frac{i\sqrt{2\gamma_1}b^{in}}{i(\omega_p - \omega_0) - \gamma}, \quad (6)$$

yields the following compact form

$$\frac{db}{d\tau} + \lambda b = \frac{c^{in}}{\omega_0}, \quad (7)$$

where  $b = B - B_\infty$  represents the difference between the mode amplitude variable and the steady state solution, while  $\lambda$  reads

$$\lambda = \frac{\gamma - i(\omega_p - \omega_0)}{\omega_0}. \quad (8)$$

By applying the methods of Gardiner and Collett introduced in Ref.<sup>35</sup> one can obtain the following input-output relation

$$b^{out} = b^{in} - i\sqrt{2\gamma_1}B, \quad (9)$$

which relates the output signal  $a_1^{out} = b^{out}e^{i\omega_p t}$  reflected off the resonator to the input signal  $a_1^{in} = b^{in}e^{-i\omega_p t}$  entering the system.

Thus, the reflection parameter  $r$  in steady state is in general given by

$$r = \frac{b^{out}}{b^{in}} = \frac{\gamma_2 - \gamma_1 - i(\omega_p - \omega_0)}{\gamma_2 + \gamma_1 - i(\omega_p - \omega_0)}, \quad (10)$$

which is obtained by substituting  $B_\infty$  of Eq. (6) in the input-output relation given by Eq. (9) and dividing by the input drive amplitude  $b^{in}$ .

### B. Heat Balance of Local Heating

The total power dissipated in the resonator  $Q_t$  is given by

$$Q_t = \hbar\omega_0 2\gamma_2 |B|^2. \quad (11)$$

Furthermore, assuming that the resonator nonlinearity is dominated by a local hot spot in the stripline resonator, and that the hot spot area is sufficiently small in order to consider its temperature  $T$  to be homogeneous, the heat balance equation reads<sup>36</sup>

$$C \frac{dT}{dt} = Q - W, \quad (12)$$

where  $C$  is the thermal heat capacity,  $Q$  is the power heating up the hot spot given by  $Q = \alpha Q_t$ , where  $0 \leq \alpha \leq 1$ , and  $W = H(T - T_0)$  is the power of the heat transfer to the coolant, which is assumed to be at temperature  $T_0$ , where  $H$  is the heat transfer coefficient.

In terms of the dimensionless time  $\tau$  and the dimensionless temperature given by

$$\Theta = \frac{T - T_0}{T_c - T_0}, \quad (13)$$

Eq. (12) reads

$$\frac{d\Theta}{d\tau} + g(\Theta - \Theta_\infty) = 0, \quad (14)$$

where the following quantities have been defined

$$g = \frac{H}{C\omega_0}, \quad (15)$$

and

$$\Theta_\infty = \frac{2\hbar\alpha\gamma_2 |B|^2}{gC(T_c - T_0)}. \quad (16)$$

Hence, the steady state solution of Eq. (14), reads

$$\Theta_{\infty 0} = \frac{2\hbar\alpha\gamma_2 |B_\infty|^2}{gC(T_c - T_0)}. \quad (17)$$

Moreover, if one further assumes that the fluctuation of  $B$  around  $B_\infty$ , is relatively small, one can rewrite Eq. (14) in the following form

$$\frac{d\theta}{d\tau} + g\theta = f, \quad (18)$$

where

$$\theta = \Theta - \Theta_{\infty 0}, \quad (19)$$

and  $f$  reads

$$f = g\Theta_{\infty 0} \left[ \frac{b}{B_\infty} + \left( \frac{b}{B_\infty} \right)^* \right]. \quad (20)$$

In general, when a hot spot is generated or alternatively diminished in the stripline, it affects the resonator parameters  $\omega_0$ ,  $\gamma_1$ ,  $\gamma_2$ ,  $\alpha$  and may induce as a result jumps in the resonance response curve. Moreover, as we have already shown in previous publications<sup>27,28</sup>, most of the nonlinear experimental results exhibited by our superconducting NbN resonators can be modeled to a very good extent by assuming a step function dependence of the resonator parameters  $\omega_0$ ,  $\gamma_1$ ,  $\gamma_2$ ,  $\alpha$  on the hot spot temperature

$$\omega_0 = \begin{cases} \omega_{0s} & \Theta < 1 \\ \omega_{0n} & \Theta > 1 \end{cases}, \quad \gamma_1 = \begin{cases} \gamma_{1s} & \Theta < 1 \\ \gamma_{1n} & \Theta > 1 \end{cases}, \quad (21)$$

$$\gamma_2 = \begin{cases} \gamma_{2s} & \Theta < 1 \\ \gamma_{2n} & \Theta > 1 \end{cases}, \quad \alpha = \begin{cases} \alpha_s & \Theta < 1 \\ \alpha_n & \Theta > 1 \end{cases}. \quad (22)$$

In addition, we have shown that, in general, while disregarding noise, the coupled equations (7) and (14) may have up to two different steady state solutions. A superconducting steady state (S) exists when  $\Theta_{\infty 0} < 1$ , or when  $E < E_s$ , where  $E_s = gC(T_c - T_0)/2\alpha_s\gamma_{2s}\hbar$ . Similarly, a normal steady state (N) exists when  $\Theta_{\infty 0} > 1$ , or when  $E > E_n$ , where  $E_n = gC(T_c - T_0)/2\alpha_n\gamma_{2n}\hbar$ .

### III. FLUCTUATIONS

In this section we assume a nonzero noise term  $c^{in}(t)$  entering the resonator, thus giving rise to fluctuations around the steady state solution.

#### A. Mode Fluctuations

In this case the solution of Eq. (7) reads

$$b(\tau) = b(0)e^{-\lambda\tau} + \frac{1}{\omega_0} \int_0^\tau c^{in}(\tau') e^{\lambda(\tau'-\tau)} d\tau'. \quad (23)$$

For relatively long times  $\gamma\tau/\omega_0 \gg 1$  one gets by using Eq. (2) a zero mean value of the mode fluctuation  $b$

$$\langle b(\tau) \rangle = 0, \quad (24)$$

whereas by using Eqs. (3), and (4) respectively, one obtains the following autocorrelation functions

$$\langle b(\tau_1) b(\tau_2) \rangle = \langle b^*(\tau_1) b^*(\tau_2) \rangle = 0, \quad (25)$$

and

$$\langle b(\tau_1) b^*(\tau_2) \rangle = \frac{G\omega_0}{2\gamma} e^{-\lambda^*|\tau_2 - \tau_1|}. \quad (26)$$

#### B. Local Heating Fluctuations

Similarly, the solution of Eq. (18) reads

$$\theta(\tau) = \langle \theta(\tau) \rangle + \Delta_\theta(\tau), \quad (27)$$

where

$$\langle \theta(\tau) \rangle = \theta(0) e^{-g\tau}, \quad (28)$$

is the mean value of  $\theta$  variable and

$$\Delta_\theta(\tau) = \int_0^\tau f(\tau') e^{g(\tau'-\tau)} d\tau', \quad (29)$$

is the deviation.

The variance of  $\theta$ , which is denoted as  $\langle \Delta_\theta^2(\tau) \rangle$ , can be derived with the use of Eqs. (29), (20), and (26). In the case of small  $\tau$ , namely the case when  $g\tau \ll 1$  and  $|\lambda|\tau \ll 1$ , one has to lowest order in  $\tau$

$$\langle \Delta_\theta^2(\tau) \rangle = \frac{g^2 \Theta_{\infty 0}^2}{|B_\infty|^2} \frac{2G\omega_0\tau^2}{\gamma}. \quad (30)$$

On the other hand, for relatively long times  $g\tau \gg 1$  one finds

$$\langle \Delta_\theta^2 \rangle = \frac{G\Theta_{\infty 0}^2}{|B_\infty|^2} \frac{g\omega_0^2}{\gamma} \frac{\gamma + g\omega_0}{(\gamma + g\omega_0)^2 + (\omega_p - \omega_0)^2}. \quad (31)$$

By taking the square of Eq. (18) one obtains

$$\zeta^2 + g \frac{d(\theta^2)}{d\tau} + g^2 \theta^2 = f^2, \quad (32)$$

where the variable  $\zeta$  is given by

$$\zeta(\tau) \equiv \frac{d\theta}{d\tau}. \quad (33)$$

Expressing  $\zeta(\tau)$  as a sum of a mean value and a deviation terms in a similar manner to Eq. (27) yields

$$\zeta(\tau) = \langle \zeta(\tau) \rangle + \Delta_\zeta(\tau). \quad (34)$$

To evaluate the variance of  $\zeta(\tau)$ , which is denoted as  $\langle \Delta_\zeta^2(\tau) \rangle$ , in the limit of relatively long times we employ Eqs. (32), (31), (20), (25), (26) and get

$$\langle \Delta_\zeta^2 \rangle = \frac{g^2 G \Theta_{\infty 0}^2}{|B_\infty|^2} \frac{\omega_0}{\gamma} \frac{(\omega_p - \omega_0)^2 + \gamma(\gamma + g\omega_0)}{(\gamma + g\omega_0)^2 + (\omega_p - \omega_0)^2}. \quad (35)$$

#### IV. ESCAPE RATE

Escape from S to N states originates from a flux at point  $\Theta = 1$  (or  $\theta = 1 - \Theta_{\infty 0}$ ) flowing from  $\Theta < 1$  to  $\Theta > 1$ , or vice versa for the case of escape from N to S states. Thus, the escape rate is given by

$$\Gamma = \omega_0 \int_0^\infty \zeta f(1 - \Theta_{\infty 0}, \zeta) d\zeta, \quad (36)$$

where  $f(\theta, \zeta)$  is the joint probability distribution function of the random variables  $\theta$  and  $\zeta$ . As was shown above, in the limit where  $g\tau \gg 1$ , the expectation values  $\langle \theta \rangle$  and  $\langle \zeta \rangle$  vanish. In general,  $f(\theta, \zeta)$  is expected to represent a joint normal distribution. Moreover,  $\theta$  and  $\zeta$  become statistically independent as the expectation value  $\langle \theta^2 \rangle$  becomes time independent. This can be readily inferred from the following relation

$$\langle \Delta_\theta \Delta_\zeta \rangle = \frac{1}{2} \frac{d\langle \theta^2 \rangle}{d\tau} - \langle \theta \rangle \langle \zeta \rangle. \quad (37)$$

Thus, by applying the previous approximations one finds

$$\Gamma = \frac{\omega_0 \exp\left[-\frac{(1-\Theta_{\infty 0})^2}{2\langle \Delta_\theta^2 \rangle}\right]}{2\pi \sqrt{\langle \Delta_\theta^2 \rangle \langle \Delta_\zeta^2 \rangle}} \int_0^\infty \zeta \exp\left(-\frac{\zeta^2}{2\langle \Delta_\zeta^2 \rangle}\right) d\zeta. \quad (38)$$

Furthermore, by evaluating the integral, substituting instead of  $G$  and  $\Theta_{\infty 0}$  (given by Eqs. (5) and (17) respectively), and using the notations

$$C = \frac{1}{2} \frac{(\gamma + g\omega_0)^2 + (\omega_p - \omega_0)^2}{g\omega_0(\gamma + g\omega_0)}, \quad (39)$$

$$\Gamma_0 = \frac{\omega_0}{2\pi} \sqrt{\frac{g[(\omega_p - \omega_0)^2 + \gamma(\gamma + g\omega_0)]}{\omega_0(\gamma + g\omega_0)}}, \quad (40)$$

one gets

$$\Gamma = \Gamma_0 \exp\left[-\frac{C(U_c - U_\infty)^2}{U_\infty k_B T_{\text{eff}}}\right], \quad (41)$$

where

$$U_\infty = \hbar\omega_0 |B_\infty|^2, \quad (42)$$

is the energy stored in the resonator corresponding to the steady state amplitude  $B_\infty$ , and

$$U_c = \hbar\omega_0 |B_c|^2, \quad (43)$$

is the mode energy corresponding to the critical amplitude  $B_c$  at which  $\Theta_{\infty 0} = 1$ , namely

$$1 = \Theta_{\infty 0} = \frac{2\hbar\alpha\gamma_2 |B_c|^2}{gC(T_c - T_0)}. \quad (44)$$

Note that typically in our NbN devices<sup>28</sup>  $\gamma/g\omega_0 \simeq 10^{-2}$ . Thus, by assuming the limit  $\gamma/g\omega_0 \ll 1$ , and the resonance case  $\omega_p = \omega_0$ , the above expression appearing in Eq. (41) reduces into

$$\Gamma = \frac{\sqrt{g\omega_0\gamma}}{2\pi} \exp\left[-\frac{1}{2} \frac{(U_c - U_\infty)^2}{U_\infty k_B T_{\text{eff}}}\right]. \quad (45)$$

#### V. STOCHASTIC RESONANCE

In order to examine experimentally the escape rate expression derived in Eq. (41), we employed stochastic resonance technique. Basically, stochastic resonance phenomenon demonstrates how a weak periodic signal, applied to a nonlinear metastable system, can be amplified at the system output with the aid of certain amount of zero-mean Gaussian white noise. The amplification of the signal occurs when a resonant cooperation is established between the small periodic signal and the white noise entering the system. In general, such a coherent interaction between the signal and the noise occurs when

the angular frequency  $\Omega$  of the signal, which periodically modulates the double-well potential of the system, becomes comparable to the escape rate of the metastable states in the presence of the white noise.

The stripline center-layer layout of the NbN resonator employed in the measurements is shown at the top-right corner of Fig. 1. The resonator was dc-magnetron sputtered on a 34 mmX 30 mmX 1 mm Sapphire substrate in an ambient gas mixture of Ar/N<sub>2</sub> at room temperature. The resonator was patterned using standard optical lithography and ion-milling. The resonator thickness was set to 2200 Å. Additional fabrication process parameters are listed in Ref.<sup>27</sup>. Whereas modeling and characterization of these nonlinear resonators are elaborated in Ref.<sup>28</sup>.

The metastable states of the system in our case, are manifested by the occurrence of jumps in the resonance line shape of the resonator. In Fig. 2 (a) we show a reflection parameter measurement of the first resonance mode of the resonator  $f_0 = \omega_0/2\pi \simeq 2.575$  GHz, which exhibits two frequency hysteresis loops forming at both sides of the resonant curve as the microwave frequency is swept in the forward and backward directions. In Fig. 2 (b) on the other hand, we show a reflected power hysteretic behavior measured at a constant frequency  $f_p = \omega_p/2\pi = 2.565$  GHz which falls within the instable region of the fundamental mode, as the input power is swept up and down. Thus, in order to drive our resonators into metastability, we have applied a coherent microwave signal at frequency  $f_p$  and input power  $P_0 = -21.5$  dBm. Moreover, in order to tune the resonator into stochastic resonance condition, we have applied a small sinusoidal forcing to the system in the form of amplitude modulation, and injected a thermal white noise with an adjustable intensity to the resonator port.

A schematic illustration of the stochastic resonance measurement setup used is depicted in Fig. 1. A continuous microwave signal at frequency  $f_p$  is amplitude modulated at frequency  $f_\Omega = \Omega/2\pi = 1$  kHz. The modulated signal which effectively modulates the height of the potential barrier is combined with a white noise and fed to the superconducting resonator. The reflected signal off the resonator on the other hand, is mixed with a local oscillator of frequency  $f_p$  and measured in the time domain using an oscilloscope. Additional information regarding stochastic resonance phenomenon measured in these nonlinear superconducting resonators is summarized in Ref.<sup>30</sup>.

### A. Escape Rate Measurement

At stochastic resonance condition, the lifetime of the metastable states becomes approximately equal to half the modulation period. Thus, assuming that the system has two metastable states designated by  $S_u$  and  $S_d$ , one obtains at this condition, one metastable state escape event each half time cycle. This is shown in Fig.

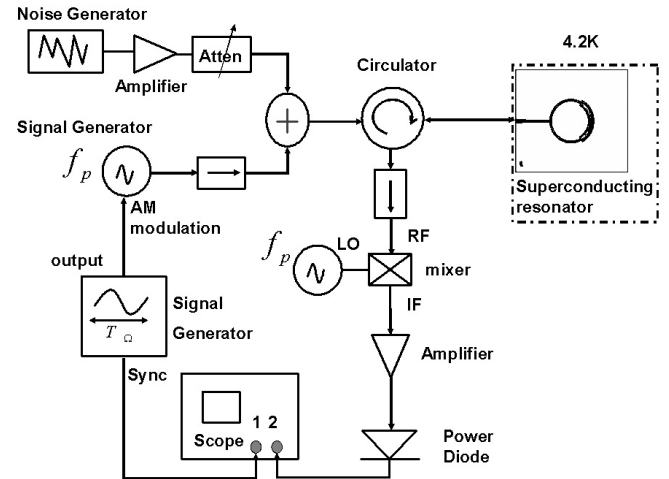


FIG. 1: Schematic block diagram of the experimental setup used in order to measure stochastic resonance. The microwave signal generator and the local oscillator at frequency  $f_p$  were phase locked. The layout of the resonator is shown at the top-right corner.

3, which shows a typical result taken in the time domain at stochastic resonance conditions, where the jumps appearing in the output signal correspond to alternating  $S_u \rightarrow S_d$  and  $S_d \rightarrow S_u$  transitions.

The blue dotted line shows the amplitude modulation signal, which modulates the escape rates  $\Gamma_1$  and  $\Gamma_2$  of the transitions  $S_d \rightarrow S_u$  and  $S_u \rightarrow S_d$  respectively. Near the minimum (maximum) points of the amplitude modulation signal the rate  $\Gamma_1$  ( $\Gamma_2$ ) obtains its largest value, which is denoted as  $\Gamma_{m1}$  ( $\Gamma_{m2}$ ). Let  $\tau_1$  ( $\tau_2$ ) be the difference between the time of the transition  $S_d \rightarrow S_u$  ( $S_u \rightarrow S_d$ ) and the time at which the corresponding escape rate obtains its largest value, namely the time at which  $\Gamma_1 = \Gamma_{m1}$  ( $\Gamma_2 = \Gamma_{m2}$ ). The probability density of the random variable  $\tau_1$  ( $\tau_2$ ) is denoted by  $f_1(\tau_1)$  ( $f_2(\tau_2)$ ).

An estimate for the escape rates  $\Gamma_{m1}$  and  $\Gamma_{m2}$  could be obtained by measuring the probability densities  $f_1(\tau_1)$  and  $f_2(\tau_2)$ . As can be seen from Eq. (A12) in the appendix,  $\Gamma_{m1}$  and  $\Gamma_{m2}$  can be estimated from the expectation value and the variance of the corresponding random variables  $\tau_1$  and  $\tau_2$ . However, a more accurate value of the prefactor  $\Gamma_m$  can be obtained by invoking Eq. (A3) and using the measured probability density function  $f(\tau)$ .

In Fig. 4 (a) and (b) we show the measured probability densities  $f_1(\tau_1)$  and  $f_2(\tau_2)$  derived from 5000 modulation cycles sampled in the time domain. The solid line in both panels represent a Gaussian function fitted to the measured probability density in each case. The transition rate  $\Gamma_1$  ( $\Gamma_2$ ) as a function of the random variable  $\tau_1$  ( $\tau_2$ ), which is found using Eq. (A3) and the Gaussian fit, is shown in the inset of Fig. 4 (a) [Fig. 4 (b)]. These plots yield also the values  $\Gamma_{m1} \simeq 4.6 \cdot 10^5$  Hz and  $\Gamma_{m2} \simeq 2.7 \cdot 10^5$  Hz for the transitions  $S_d \rightarrow S_u$  and  $S_u \rightarrow S_d$

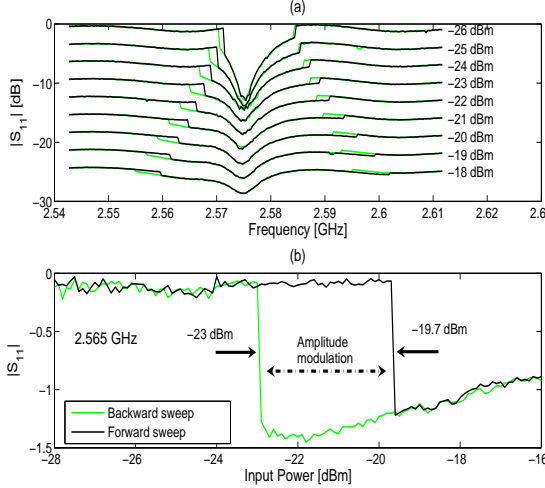


FIG. 2: (Color online). (a) Forward and backward frequency sweeps applied to the first mode of the resonator at  $\sim 2.575$  GHz. The sweeps exhibit hysteresis loops at both sides of the resonance line shape. The plots corresponding to different input powers were shifted by a vertical offset for clarity. (b) Reflected power hysteresis measured at a constant angular frequency of  $\omega_p = 2\pi \cdot 2.565$  GHz which resides within the left-side metastable region of the resonance. For both plots the black (dark) line represents a forward sweep whereas the green (light) line represents a backward sweep.

respectively.

## B. Discussion

In order to obtain theoretical estimates for the escape rates  $\Gamma_{m1}$  and  $\Gamma_{m2}$  corresponding to the  $S_d \rightarrow S_u$  and  $S_u \rightarrow S_d$  transitions respectively we rewrite Eq. (41) in terms of the feedline input power  $P_{in}$  at the extremum of the AM modulation, and the power difference  $\Delta P_{in} \equiv P_c - P_{in}$ , where  $P_c$  is the critical input power, which is proportional to  $U_c$ ,

$$\Gamma_m = \Gamma_0 \exp \left[ -C \left( \frac{\Delta P_{in}}{P_{in}} \right)^2 \frac{U_\infty}{k_B T_{\text{eff}}} \right], \quad (46)$$

where, according to Eq. (1), the following holds

$$U_\infty = \frac{P_{in} (1 - |r|^2)}{2\gamma}. \quad (47)$$

Estimates for the model parameters corresponding to both  $S_d \rightarrow S_u$  and  $S_u \rightarrow S_d$  transitions are summarized in Table 1. Estimates for the coupling parameter  $\gamma$  corresponding to the  $S_u$  and the  $S_d$  states have been extracted indirectly by fitting Eq. (10) to the measured  $r$  vs.  $\omega_p$  curves in the vicinity of the resonance<sup>37</sup>.

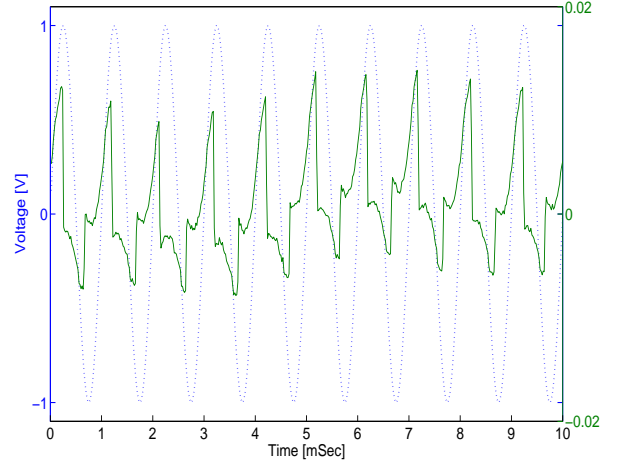


FIG. 3: (Color Online). A typical snapshot of the time domain as the resonator is tuned into stochastic resonance condition. The solid (green) line represents the reflected modulated signal, corresponding to ten modulation cycles out of 5000 employed in the analysis. The dotted (blue) sinusoidal line represents the modulation signal applied to the microwave signal generator.

TABLE I: Calculated and Measured Model Parameters

	$S_d \rightarrow S_u$	$S_u \rightarrow S_d$
$g [10^{-3}]$	1.56	1.56
$\gamma [\text{MHz}]$	37.6	18.6
$P_c [\text{dBm}]$	-23	-19.6
$\Delta P_{in} [10^{-6} \text{W}]$	0.12	1.2
$ r ^2$	0.55	0.8
$k_B T_{\text{eff}} [\text{fW/Hz}]$	1.4	1.4
$\Gamma_0 [\text{Hz}]$	$8 \cdot 10^6$	$8.3 \cdot 10^6$
$\Gamma_m [\text{Hz}] \text{ (calc.)}$	$7.8 \cdot 10^6$	$1.9 \cdot 10^6$
$\Gamma_m [\text{Hz}] \text{ (meas.)}$	$4.6 \cdot 10^5$	$2.7 \cdot 10^5$

Whereas, the cooling parameter  $g$ , which is defined in Eq. (15), has been estimated using experimentally measured material properties of NbN<sup>38,39,40</sup>, yielding the value  $g \simeq 1.56 \cdot 10^{-3}$  (see Refs.<sup>28,32</sup>). Employing these estimates together with the experimental values of  $P_c$ ,  $\Delta P_{in}$ ,  $r$ , and substituting in Eq. (46) yield a rough estimate for the escape rates  $\Gamma_{m1} \simeq 7.8 \cdot 10^6$  Hz and  $\Gamma_{m2} \simeq 1.9 \cdot 10^6$  Hz for the  $S_d \rightarrow S_u$  and the  $S_u \rightarrow S_d$  transitions respectively.

The discrepancy in the values of the escape rates obtained using the theoretical model as opposed to the ones extracted from the experimental data (by about an order of magnitude) can be attributed most likely to the

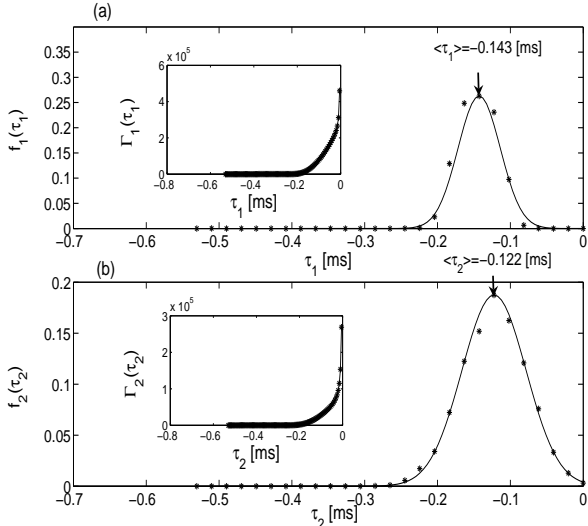


FIG. 4: Gaussian probability density functions  $f_1(\tau_1)$  and  $f_2(\tau_2)$  fitted to the experimental data which correspond to the  $S_d \rightarrow S_u$  transition in panel (a) and to the  $S_u \rightarrow S_d$  transition in panel (b). The escape rates  $\Gamma_1$  and  $\Gamma_2$  associated with both transitions are plotted in the insets of panels (a) and (b) respectively as a function of the random time variables  $\tau_1$  and  $\tau_2$  according to Eq. (A3).

accumulated errors in the estimated values of the model parameters which have been evaluated indirectly. For example, the  $g$  parameter depends among others on the geometry of the hot spot and the thermal properties of the deposited NbN film, which are not known precisely. Moreover, inaccuracies in the coupling factor  $\gamma$  may result due to some approximations, which were employed in the fitting procedure<sup>37</sup>.

## VI. SUMMARY

In conclusion, a noise-activated escape rate expression was derived for the case of a nonlinear superconducting resonator having a local-thermal instability. Moreover, stochastic resonance measurements were exploited to experimentally determine the escape rate. A partial agreement is found between the theoretical and the experimental results.

## APPENDIX A: TRANSITION LIFETIME

Consider a system which has in general two metastable states designated by  $S_a$  and  $S_b$  and assume that at time  $t = -t_0$  the system is in state  $S_b$ , where  $t_0 > 0$ . The transition rate  $\Gamma$  of the process  $S_b \rightarrow S_a$  depends on an externally applied time varying parameter  $p(t)$ . Further assume that for  $p$  close to some fixed value  $p_m$  the tran-

sition rate is given approximately by

$$\Gamma(p) = \Gamma_m \exp\left(-\kappa^2 \frac{p - p_m}{p_m}\right), \quad (A1)$$

where both  $\Gamma_m$  and  $\kappa$  are positive constants.

The probability distribution function  $F(\tau)$  for a transition of the kind  $S_b \rightarrow S_a$  to take place within the time interval  $(-t_0, \tau)$  is given by

$$F(\tau) = \int_{-t_0}^{\tau} f(t) dt, \quad (A2)$$

where  $f(\tau)$  is the corresponding probability density. By definition, the following holds

$$\frac{f(\tau)}{1 - F(\tau)} = \Gamma[p(\tau)]. \quad (A3)$$

The initial condition  $F(-t_0) = 0$  and Eq. (A3) yield

$$f(\tau) = \Gamma[p(\tau)] \exp\left(-\int_{-t_0}^{\tau} \Gamma[p(t)] dt\right). \quad (A4)$$

Further assume the case where at time  $t = 0$  the function  $p(t)$  obtains a local minimum  $p(0) = p_m$ . Near  $t = 0$  one has

$$p(t) = p_m (1 + \Omega^2 t^2) + O(t^3). \quad (A5)$$

Thus, in the vicinity of  $t = 0$  Eq. (A1) becomes

$$\Gamma(t) = \Gamma_m \exp(-\kappa^2 \Omega^2 t^2), \quad (A6)$$

and the following holds

$$f(\tau) = \Gamma_m \exp\left(-\kappa^2 \Omega^2 \tau^2 - \sqrt{\pi} \frac{\Gamma_m}{\kappa \Omega} \frac{\text{erf}(\kappa \Omega \tau) + \text{erf}(\kappa \Omega t_0)}{2}\right). \quad (A7)$$

Keeping terms up to second order in  $\kappa \Omega \tau$  and assuming the case where

$$\left(-\kappa \Omega t_0 + \frac{\Gamma_m}{2 \kappa \Omega}\right)^2 \gg 1, \quad (A8)$$

allow approximating the probability density  $f(\tau)$  by

$$f(\tau) = \frac{\Omega \kappa}{\sqrt{\pi}} \exp\left[-\kappa^2 \Omega^2 \left(\tau + \frac{\Gamma_m}{2 \kappa^2 \Omega^2}\right)^2\right]. \quad (A9)$$

In this approximation the random variable  $\tau$  has a normal distribution function with a mean value

$$\mu_{\tau} = -\frac{\Gamma_m}{2 \kappa^2 \Omega^2}, \quad (A10)$$

and a variance

$$\sigma_\tau^2 = \frac{1}{2\kappa^2\Omega^2} . \quad (\text{A11})$$

Whereas, the parameters  $\Gamma_m$  and  $\kappa$ , are given by

$$\Gamma_m = -\frac{\mu_\tau}{\sigma_\tau^2} , \quad (\text{A12})$$

and

$$\kappa^2 = \frac{1}{2\sigma_\tau^2\Omega^2} . \quad (\text{A13})$$

## ACKNOWLEDGMENT

This work was supported by the German Israel Foundation under grant 1-2038.1114.07, the Israel Science Foundation under grant 1380021, the Deborah Foundation, the Poznanski Foundation, and MAFAT.

\* Electronic address: baleegh@tx.technion.ac.il

<sup>1</sup> P. Hänggi, P. Talkner, and M. Borkovec, Rev. Mod. Phys. **62**, 251 (1990).

<sup>2</sup> *Activated Barrier Crossing; Applications in Physics, Chemistry, and Biology*, edited by G. R. Fleming and P. Hänggi (World Scientific, Singapore, 1993).

<sup>3</sup> E. H. Serpersu and T. Y. Tsong, J. Membr. Biol. **74**, 191 (1983).

<sup>4</sup> T. A. Fulton and L. N. Dunkleberger, Phys. Rev. B **9**, 4760 (1974).

<sup>5</sup> M. Büttiker, E. P. Harris, and R. Landauer, Phys. Rev. B **28**, 1268 (1983).

<sup>6</sup> W. Wernsdorfer, E. B. Orosco, K. Hasselbach, A. Benoit, B. Barbara, N. Demony, A. Loiseau, Phys. Rev. Lett. **78**, 1791 (1997).

<sup>7</sup> R. H. Koch, G. Grinstein, G. A. Keefe, Yu Lu, P. L. Trouiloud, W. J. Gallagher, and S. S. P. Parkin, Phys. Rev. Lett. **84**, 5419 (2000).

<sup>8</sup> E. B. Myers, F. J. Albert, J. C. Sankey, E. Bonet, R. A. Buhrman, and D. C. Ralph, Phys. Rev. Lett. **89**, 19680 (2002).

<sup>9</sup> C. Stambaugh and H. B. Chan, Phys. Rev. B **73**, 172302 (2006).

<sup>10</sup> J. S. Aldridge and A. N. Cleland, Phys. Rev. Lett. **94**, 156403 (2005).

<sup>11</sup> R. L. Badzey, G. Zolfagharkhani, A. Gaidarzhy, and P. Mohanty, Appl. Phys. Lett. **86**, 023106 (2005).

<sup>12</sup> B. J. Keay, S. J. Allen, Jr., J. Galán, J. P. Kaminski, K. L. Campman, A. C. Gossard, U. Bhattacharya, and M. J. W. Rodwell, Phys. Rev. Lett. **75**, 4098 (1995).

<sup>13</sup> H. A. Kramers, Physica **7**, 284 (1940).

<sup>14</sup> M. I. Dykman and M. A. Krivoglaz, Physica **104A**, 408 (1980).

<sup>15</sup> V. I. Mel'nikov and S. V. Meshkov, J. Chem. Phys. **85**, 1018 (1986).

<sup>16</sup> M. I. Dykman, I. B. Schwartz and M. Shapiro, Phys. Rev. E **72**, 021102 (2005).

<sup>17</sup> R. Graham and T. Tél, Phys. Rev. A **31**, 1109 (1985).

<sup>18</sup> R. S. Maier and D. L. Stein, SIAM J. Appl. Math. **57**, 752 (1997).

<sup>19</sup> D. Ryvkine, M. I. Dykman, and B. Golding, Phys. Rev. E **69**, 061102 (2004).

<sup>20</sup> J. Lehmann, P. Reimann, and P. Hänggi, Phys. Rev. E **62**, 6282 (2000).

<sup>21</sup> M. I. Dykman, D. G. Luchinsky, R. Mannella, P. V. E. McClintock, N. D. Stein, and N. G. Stocks, Phys. Rev. E **49**, 1198 (1994).

<sup>22</sup> L. Gammaitoni, P. Hänggi, P. Jung, and F. Marchesoni, Rev. Mod. Phys. **70**, 223 (1998).

<sup>23</sup> H. S. Wio, P. Colet, M. S. Miguel, L. Pesquera, and M. A. Rodriguez, Phys. Rev. A **40**, 7312 (1989).

<sup>24</sup> S. J. B. Einchcomb and A. J. McKane, Phys. Rev. E **51**, 2974 (1995).

<sup>25</sup> P. Hänggi, J. Stat. Phys. **42**, 105 (1986).

<sup>26</sup> O. A. Tretiakov, T. Gramespacher, and K. A. Matveev, Phys. Rev. B **67**, 073303 (2003); O. A. Tretiakov and K. A. Matveev, Phys. Rev. B **71**, 165326 (2005).

<sup>27</sup> B. Abdo, E. A.-Segev, O. Shtempluck, and E. Buks, cond-mat/0501114 to be published in IEEE Trans. Appl. Supercond.

<sup>28</sup> B. Abdo, E. A.-Segev, O. Shtempluck, and E. Buks, Phys. Rev. B **73**, 134513 (2006).

<sup>29</sup> B. Abdo, E. A.-Segev, O. Shtempluck, and E. Buks, Appl. Phys. Lett. **88**, 022508 (2006).

<sup>30</sup> B. Abdo, E. A.-Segev, O. Shtempluck, and E. Buks, cond-mat/0606555.

<sup>31</sup> E. A.-Segev, B. Abdo, O. Shtempluck, and E. Buks, cond-mat/0607259.

<sup>32</sup> E. A.-Segev, B. Abdo, O. Shtempluck, and E. Buks, cond-mat/0607261.

<sup>33</sup> E. A.-Segev, B. Abdo, O. Shtempluck, and E. Buks, cond-mat/0607262.

<sup>34</sup> B. Yurke and E. Buks, arXiv:quant-ph/0505018 (3 May 2005).

<sup>35</sup> C. W. Gardiner and M. J. Collett, Phys. Rev. A **31**, 3761 (1985).

<sup>36</sup> A. VI. Gurevich and R. G. Mints, Rev. Mod. Phys. **59**, 941 (1987).

<sup>37</sup> B. Abdo, E. A.-Segev, O. Shtempluck, and E. Buks, cond-mat/0501236 to be published in IEEE Trans. Appl. Supercond.

<sup>38</sup> M. W. Johnson, A. M. Herr, and A. M. Kadin, J. Appl. Phys. **79**, 7069 (1996).

<sup>39</sup> A. M. Kadin and M. W. Johnson, Appl. Phys. Lett. **69**, 3938 (1996).

<sup>40</sup> K. Weiser, U. Strom, S. A. Wolf, and D. U. Gubser, J. Appl. Phys. **52**, 4888 (1981).